KARYA ILHAM PUBLISHING
CONNECTING MINDS, BRIDGING IDEAS, INSPIRING READERS

Advances in Fluid, Heat and Materials Engineering

Journal homepage:
https://karyailham.com.my/index.php/afhme/index
ISSN: 3083-8134

Modelling of Flow Behaviour in the Curvature of Helical Coil

Lau Ming Yao[1], Ishkrizat Taib[1,*]

[1] Department of Mechanical Engineering, Faculty of Mechanical and Manufacturing Engineering, Universiti Tun Hussein Onn Malaysia, 86400 Parit Raja, Johor, Malaysia

ARTICLE INFO

Article history:
Received 25 April 2026
Received in revised form 10 May 2026
Accepted 3 June 2026
Available online 30 June 2026

ABSTRACT

Helical coils are widely utilized in industrial heat exchangers and chemical reactors due to their compact design and superior mixing capabilities compared to straight pipes. However, the complex secondary flow patterns induced by centrifugal forces create significant challenges in predicting hydraulic performance and energy requirements across different flow regimes. This research addresses the problem of accurately characterizing the transition from viscous-dominated laminar flow to inertia-dominated turbulence within curved geometries. The purpose of this study is to evaluate the influence of varying Reynolds numbers on flow topology, velocity and pressure drop characteristics. The investigation was conducted using a three-dimensional numerical simulation approach in ANSYS Fluent 2026 R1. A strong methodology was employed, featuring an unstructured patch conforming tetrahedral mesh evaluated across three distinct element resolutions to establish a Grid Independence Test (GIT). High velocity gradients adjacent to the tube walls were resolved using structured inflation layer boundaries. Steady-state simulations were executed at a fixed inlet mass flow rate of 0.01kg/s, utilizing a laminar viscous solver for low velocities, a three-equation Transition k-kl-omega model for transitional regions and a four-equation Shear Stress Transport (SST) k-omega model for fully developed turbulent environments. Quantitative results from the mesh validation show that the medium mesh resolution with 5mm element size successfully achieved numerical independence, which preserving a stable solution with a negligible pressure drop error margin of less than 3% compared to the fine mesh at 4mm while optimizing computational time. Hydrodynamic extractions reveal that under laminar conditions (Re < 2300), the viscous forces effectively suppress fluid fluctuations, which resulting in a maximum velocity magnitude of 7.806×10^{-3}m/s at the central core. Conversely, operating under transition (Re=4000) and turbulent (Re > 10,000) conditions triggers strong centrifugal fields that force the high-velocity core outward, successfully establishing counter-rotating Dean vortices. While the laminar regime maintains a steady, linear pressure distribution along the 500mm coil length, the onset of turbulent secondary flow patterns causes an aggressive, non-linear pressure drop concentrated near the inlet boundary. The study concludes that while the highly energetic turbulent regime offers optimal structural fluid mixing, the laminar regime remains the most energy-efficient configuration for primary fluid transport, providing a precise technical baseline for the geometric design and pumping optimization of helical piping networks.

Keywords:
Helical coil; CFD simulation; grid independence test; pressure drop; flow regimes

[*] *Corresponding author.*
E-mail address: iszat@uthm.edu.my

https://doi.org/10.37934/afhme.9.1.1927a

1. Introduction

Unlike flow in linear pipes, the curvature of the helical coil introduces a centrifugal force that acts upon the fluid, which causing the high velocity core to travel toward the outer wall of the tube [1]. This radial displacement generates a characteristic secondary flow pattern, demonstrating as a pair of counter-rotating vortex cells known as Dean vortices [2]. These vortices significantly enhance radial mixing and destabilize the boundary layers, which contributes to a substantial increase in the convective heat transfer coefficient. The transition between flow regimes in this helical geometry is notably more complex than in straight pipes, as the curvature exerts a stabilizing effect that delays the beginning of the turbulence flow [3]. This stabilization leads to three distinct flow regimes which are laminar, transitional and turbulent where each is characterized by varying levels of vortex intensity and pressure drop [4].

The internal fluid flow through helically coiled pipes represents a fundamental area of study in thermal engineering due to its compact design and greater efficiency in heat and mass transfer compared to straight pipe geometries [5]. Consequently, the critical Reynolds number for the transition from laminar to turbulent flow in helical coils is typically much higher than the standard Re = 2300 observed in straight pipes [6]. By evaluating the flow behavior across a range of Reynolds numbers [7,8], this research characterizes the pressure drop between the inlet and outlet along with velocity profiles and their impact on hydraulic performance. To achieve a validated understanding of these dynamics, this study establishes a high-fidelity numerical investigation using a three-dimensional finite volume approach in ANSYS Fluent 2026 R1. The computational workflow prioritizes exact geometric modeling and rigorous mesh control to ensure the solution accuracy [9].

The physical domain represents a precision helical coil with a constant pitch of 50mm and a total axial length of 500mm, generated via a continuous profile sweep in ANSYS Design Modeler. To guarantee that the numerical solutions are completely free from spatial discretization errors, a Grid Independence Test (GIT) was executed across three distinct spatial resolutions [2,10], using patch-conforming tetrahedral elements which includes a coarse mesh density of element size at 32.692 mm, a medium mesh density of 5mm and an fine mesh density of 4mm. High-velocity gradients adjacent to the bounding pipe walls are controlled via structured inflation layers along the boundary surfaces to accurately capture boundary layer growth [11]. The numerical experiments evaluate steady state fluid behaviors under a fixed inlet mass flow rate of 0.01kg/s [11,12]. The fluid physics are isolated using a standard laminar viscous model for low velocities (Re < 2300), then a three-equation Transition k-kl-omega model for transitional fields (Re approximate at 4000) and a four-equation Shear Stress Transport (SST) k-omega model for fully developed turbulent states (Re > 10000), hence ensuring appropriate mathematical closure across all tested environments [13].

The principal results extracted from these numerical simulations provide a detailed and continuous mapping of the velocity contours and pressure gradients defining for each flow regime. Structural verification confirmed that the medium mesh density with 5mm element size was successfully achieved the complete numerical independence, which shows an error margin of less than 3% relative to the fine mesh layout while significantly optimizing the computational resource costs and time. Hydrodynamic extractions show that under low Reynolds numbers, the laminar fields maintain stable and non-crossing streamlines where viscous forces successfully diminish physical disturbances, recording a maximum core velocity magnitude of 7.806×10^{-3}m/s. Upon moving into the transitional and turbulent regions, the strong centrifugal force fields alter the core pathlines. The turbulent streamlines demonstrate significant cross-sectional dispersion, which indicating highly energetic fluid interactions and the presence of fully formed counter-rotating Dean vortices. This flow transformation deeply influences the hydraulic performance, while the laminar pressure drop demonstrates a steady and linear energy dissipation across the 500mm coil length, the turbulent regime exhibits an aggressive and non-linear pressure drop concentrated near the inlet boundary.

This computational fluid dynamics study successfully characterized the complex flow phenomena within a helical coil across laminar, transition and turbulent regimes. The major conclusions drawn from this research confirm that while a fully developed turbulent flow regime delivers exceptional radial mixing and high thermal hydraulic performance, it demands a massive hydraulic compromise due to a steep and non-linear increase in the pressure drop [12-14]. Conversely, the structured laminar flow regime provides the highest energy conservation efficiency for primary fluid transport applications. By validating grid independence and matching visualise vortex developments directly with quantified pressure drops, this study provides a dependable framework which enabling thermal engineers to achieve an optimized design balance between heat transfer enhancement and pumping power requirements.

2. Methodology

2.1 Geometry and Computational Domain

The geometry for this study was developed using ANSYS Design Modeler, with the 3D drawing as shown in Figure 1. The computational domain consists of a helical coil model which was constructed using a sweep operation along a helical path defined by specific pitch and helix diameter of 50mm with a total length of 500mm. This geometric configuration is essential for capturing the centrifugal forces that drive secondary flow patterns [15].

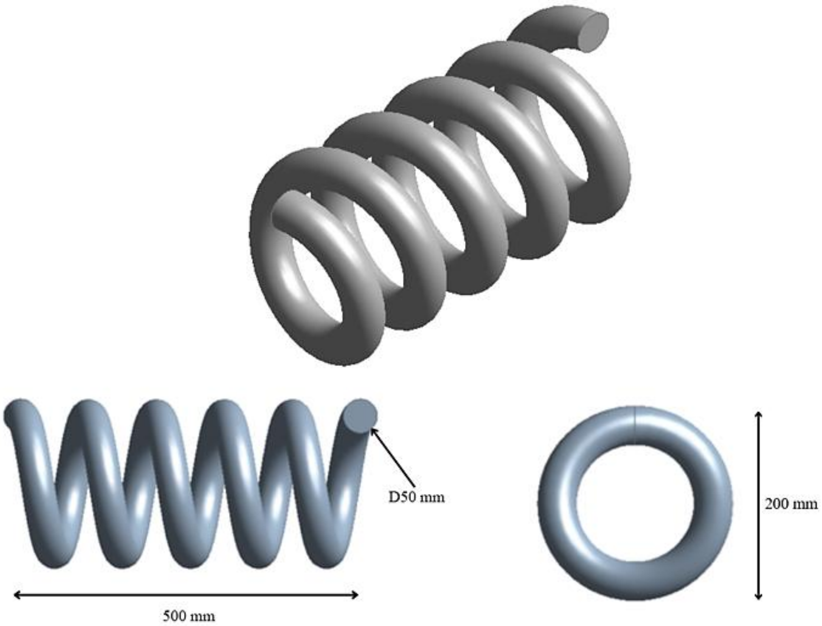

Fig. 1. 3D drawing of helical coil using ANSYS design modeler

2.2 Computational Grids and Meshing Strategy

The meshing process was conducted within the ANSYS Meshing module, utilizing a Patch Conforming Method to ensure the complex curvature of the coil was accurately captured [15,16]. Then the grid proceed with an unstructured tetrahedral mesh as show in Figure 2 was applied to the main fluid body to accommodate the helical curvature, along with the zoom view of the tetrahedral meshing. Besides that, the use of inflation layers at the pipewall boundary is a standard requirement for the simulation to capture high-velocity gradients near the wall. The named selection was done after the mesh had been created, where three primary named selections were defined for boundary condition application: which including inlet, outlet and pipewall [17].

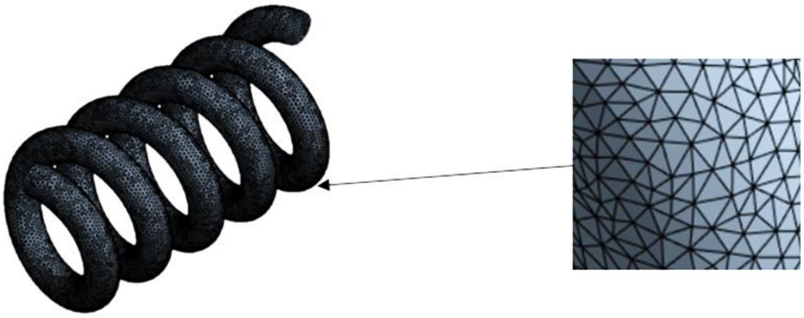

Fig. 2. Tetrahedral meshing of helical coil using patch confirming method

2.3 Boundary Conditions and Physics Setup

The numerical simulations were performed using the ANSYS Fluent pressure-based solver under steady-state conditions [18]. Inlet which is defined as a velocity inlet with the mass flow rate of 0.01kg/s, where values were calculated to correspond to the three-target model of Reynolds numbers as to be compared which include: Laminar (Re < 2,300), Transition (Re approximate=4,000), and Turbulent (Re >10000). Then at the outlet boundary condition is set as a pressure outlet with a gauge pressure of 0 Pa. The pipewall was assigned as a no-slip boundary condition. While for the viscous models to be made comparison for the study, the laminar model was utilized for low Re cases, while the transition k-kl-omega model and k-omega SST model were selected for the transitional and turbulent cases respectively. In addition, the gravitational acceleration was enabled in the Z-direction of -9.81m/s^2 to account for potential buoyancy effects if thermal variations were introduced.

2.4 Grid Independence Test

Evidence of numerical convergence was established by monitoring the data result of the outlet velocity and pressure drop. Convergence was considered successful when monitoring plots for outlet velocity and pressure drop showed no further fluctuations over three hundred iterations performed [19]. The accuracy of the solutions was validated through the GIT, ensuring that the final results were independent of the computational grid [20]. This is carried out by changing the element size from default (32.692 mm), 5 mm, and 4 mm hence to increase the nodes number of mesh. By comparing the pressure drop between the inlet and outlet across the three mesh resolutions, a medium mesh density of 5 mm element size was identified as the optimal grid, as it provided a stable solution with a negligible error margin within less than 3% compared to the fine mesh.

3. Results and Discussions

3.1 Grid Independence Test (GIT) and Convergence

Before analyzing the flow physics, a grid independence test (GIT) was performed to ensure that the numerical results were not biased by the mesh resolution. Three mesh densities of coarse (32.692 mm), medium (5 mm), and fine (4 mm) element size were evaluated using the pressure drop as the primary monitoring variable as in Table 1.

Table 1
Grid independence test result

Mesh type	Nodes numbers	Elements number	Pressure drop (Pa)	Percentage difference
Coarse	21438	97602	0.19385	-
Medium	62991	306250	0.19531	0.008
Fine	105549	524285	0.19905	0.027

As observed in the data from Table 1, the coarse mesh configuration of 97602 elements recorded a total pressure drop of 0.19385 Pa, which shifted to 0.19531 Pa for the medium mesh with 306250 elements, and finally stabilized at 0.19905 Pa for the fine mesh with 524285 elements. Refining the grid from the coarse to the medium density captures a necessary adjustment in secondary flow behaviors, whereas further refinement from the medium to the fine layout produces a negligible pressure drop variance differences of only 1.9%. Because this relative difference falls well below the standard engineering threshold of 3.0% for reliable engineering validation, the solution has achieved complete numerical convergence.

Consequently, the medium mesh configuration was selected as the optimal computational grid for all subsequent simulations, which successfully balancing high predictive accuracy with computational resource and time efficiency. Convergence was further validated by monitoring scaled residuals as in Figures 3(a) and 3(b), indicating a stable and mathematically comprehensive solution.

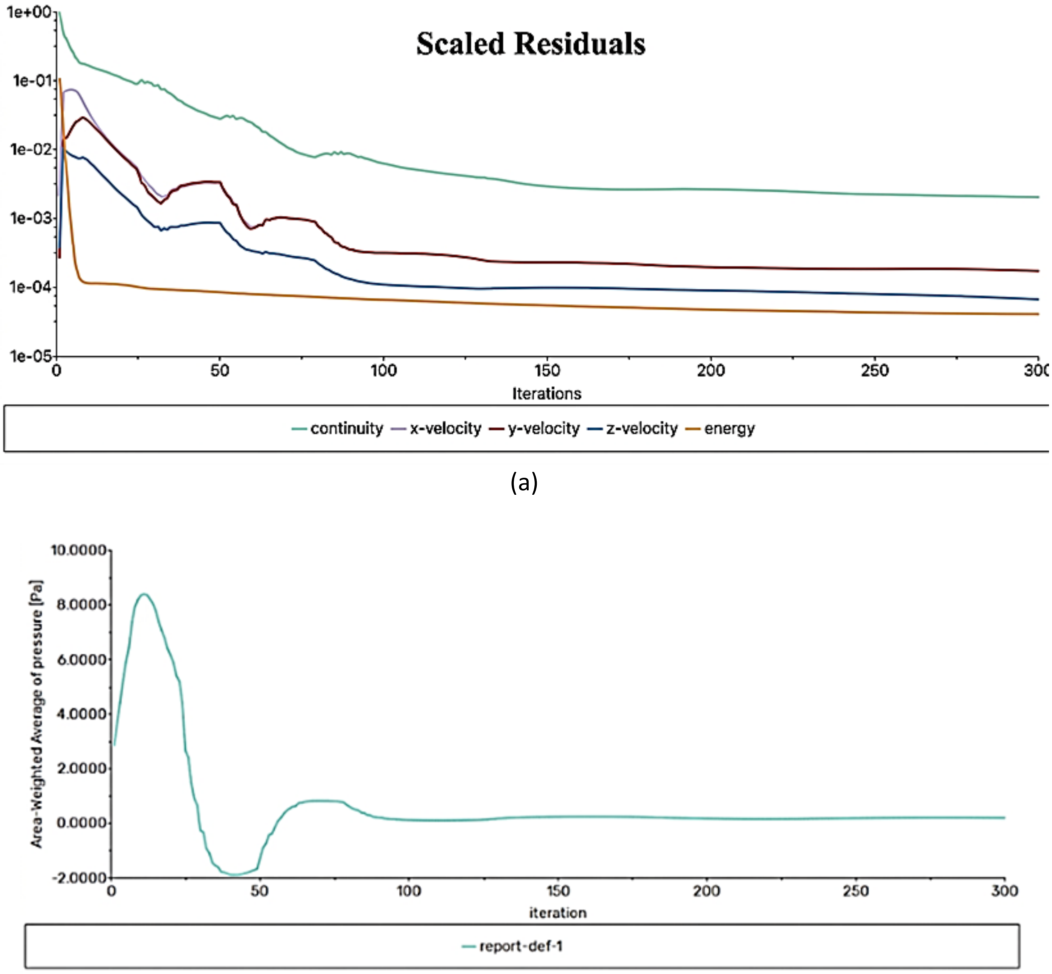

(b)

Fig. 3. Convergence monitoring plots (a) Residual (b) Pressure drop

3.2 Analysis of Velocity Contours and Flow Regimes

The velocity contour and flow regimes is shown in Figure 4. The laminar results display highly structured, steady streamlines that follow a predictable helical path with minimal crossing. In this regime, the velocity magnitude remains relatively low, peaking at 7.806(10^3) m/s in the core, while the fluid particles maintain a distinct separation, indicating that viscous forces are dominant enough to suppress random fluctuations.As the flow moves into the transition regime, the streamlines begin to show signs of increased complexity and interaction. While the general helical structure is preserved, the path lines appear slightly more tightly wound or bundled, which is a visual indicator of the fluid overcoming initial viscous stabilization to begin more intensive mixing.

In the turbulence regime, the streamlines demonstrate a more chaotic distribution despite following the same global helical path. The color mapping across all three images remains consistent for direct comparison, showing that the high-velocity core which indicated by the red regions is consistently maintained, but the turbulent streamlines exhibit a greater degree of lateral dispersion. This indicates that the centrifugal forces are effectively driving the fluid into a high-mixing state, which is the primary reason for the superior heat transfer capabilities of helical coils in industrial applications.

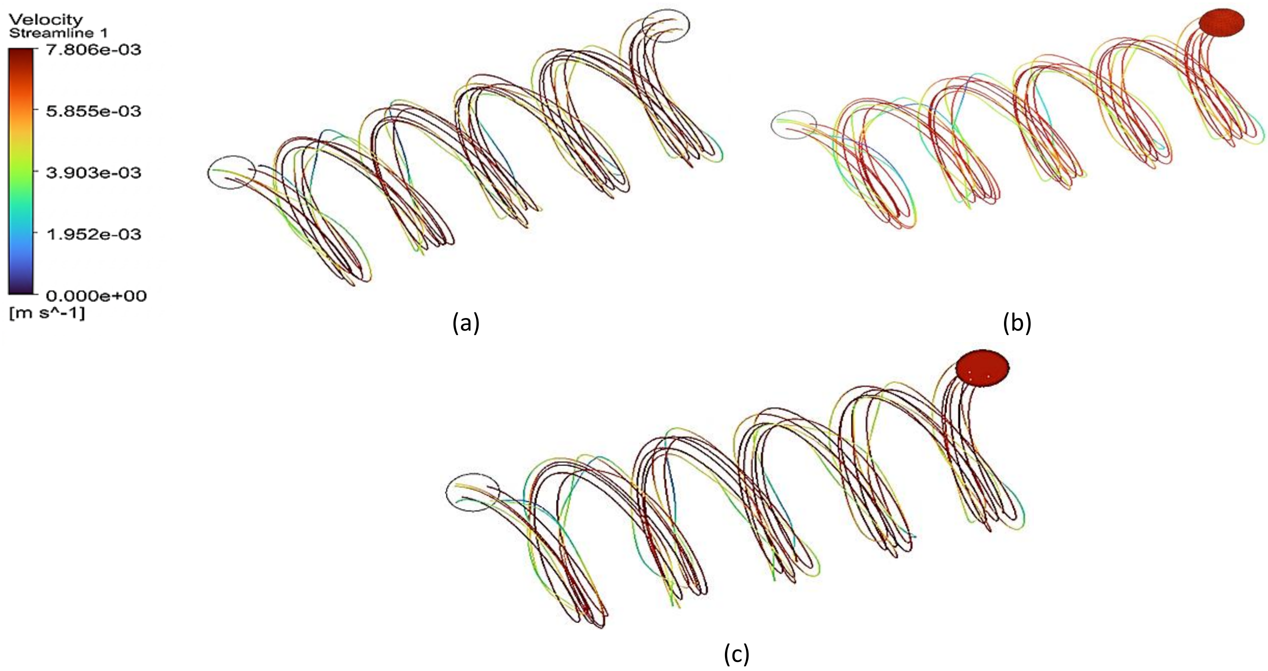

Fig. 4. Velocity contour and flow regimes across helical tube (a) Laminar (b) Transition (c) Turbulent

3.3 Analysis of Pressure Contours

The pressure contours comparison is shown in Figure 5. The comparative pressure distribution across the laminar, transition and turbulence regimes illustrates the cost of fluid motion in a curved geometry. In all three cases, the highest pressure is located at the inlet, while the pressure gradually decreases toward the outlet. In laminar regime, the pressure drop appears steady and linear. The streamlines transition smoothly from red to yellow and green, indicating a predictable dissipation of energy primarily due to viscous friction against the pipe walls.

In transition regime, there is a noticeable shift in the color gradient compared to the laminar case. The transition to lower pressure of green-blue tones occurs slightly earlier along the coil's length.

This suggests that the onset of secondary flow instabilities is beginning to consume more hydraulic energy than pure laminar flow. In turbulence regime, the pressure gradient is the most aggressive in this regime. The rapid transition from the high-pressure inlet to lower-pressure regions in light green and cyan tone across the streamlines indicates significant energy loss.

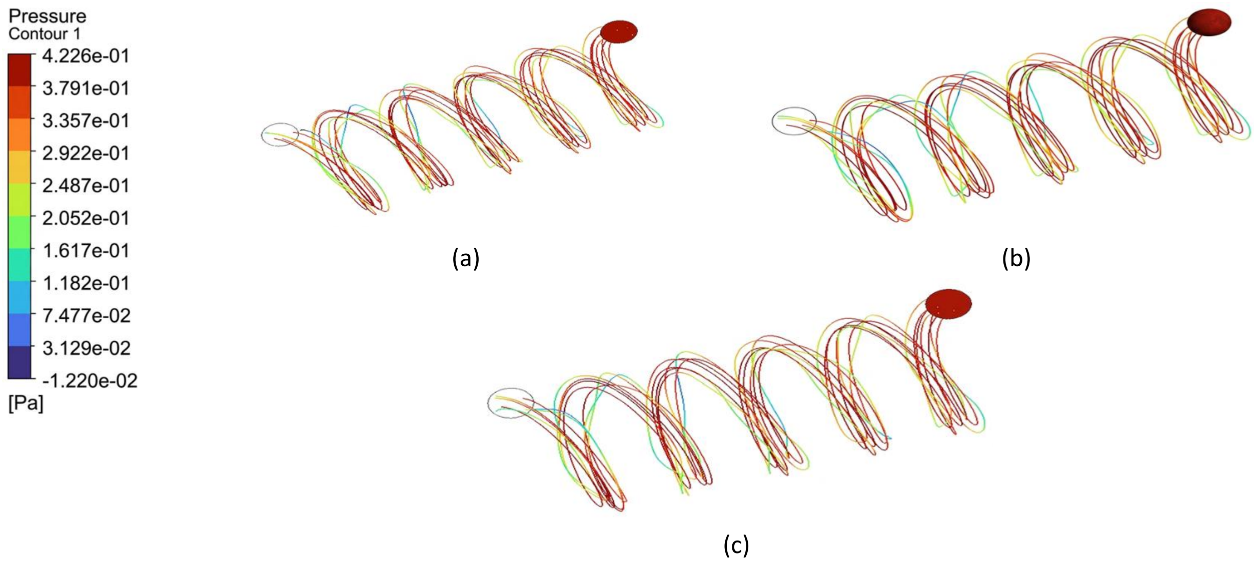

Fig. 5. Pressure contour across the helical tube (a) Laminar (b) Transition (c) Turbulent

3.4 Analysis of Flow Dynamics

The flow dynamics within the helical coil are dominated by the interaction between the primary longitudinal flow and the secondary radial flow. As visualized in the turbulence streamlines, the fluid particles follow a complex spiral path, driven by the centrifugal force that acts on the high-velocity core. This force creates a pressure imbalance that pushes the fluid toward the outer wall. In the laminar regime, these vortices are stable and symmetric, while in the turbulent regime, the vortices become highly energetic and chaotic. This intensified mixing significantly enhances the momentum exchange between the core and the wall, which is visually evidenced by the rapid color transitions in the pressure contours.

4. Conclusions

In conclusion, this computational fluid dynamics study successfully characterized the complex flow phenomena within a helical coil across laminar, transition and turbulent regimes. The simulation results, validated through a rigorous Grid Independence Test and converged residuals, demonstrate that the coil's curvature induces a significant centrifugal force that shifts the high-velocity core toward the outer wall. This displacement triggers the formation of secondary flow structures, known as Dean vortices, which become increasingly chaotic as the Reynolds number increases from the structured laminar state to fully developed turbulence. While the turbulent regime exhibits the highest mixing efficiency and enhanced momentum exchange, it simultaneously results in a non-linear increase in pressure drop, as evidenced by the aggressive gradients in the pressure contours. The high degree of correlation between the visual flow patterns and established practical theories confirms the reliability of the chosen k-omega SST turbulence model and the overall numerical methodology. Ultimately, these findings provide a strong technical basis for optimizing fluid flow in helical coil, balancing the benefits of intensified mixing against the increased hydraulic energy requirements.

References

[1] Che, Shuai, David Breitenmoser, Yuriy Yu Infimovskiy, Annalisa Manera, and Victor Petrov. "CFD simulation of two-phase flows in helical coils." *Frontiers in Energy Research* 8 (2020): 65. https://doi.org/10.3389/fenrg.2020.00065

[2] Saffar, Yeganeh, Sina Kashanj, David S. Nobes, and Reza Sabbagh. "The physics and manipulation of dean vortices in single-and two-phase flow in curved microchannels: A review." *Micromachines* 14, no. 12 (2023): 2202. https://doi.org/10.3390/mi14122202

[3] Wang, Ningyuan, Yu Bian, Deqi Chen, Haidong Liu, Hanzhou Liu, and Shanshan Bu. "Experimental study on flow-induced vibration under laminar flow and turbulent flow transition state in helical coiled tube." *Progress in Nuclear Energy* 173 (2024): 105244. https://doi.org/10.1016/j.pnucene.2024.105244

[4] Gupta, Ritu, R. K. Wanchoo, and T. R. M. Jafar Ali. "Laminar flow in helical coils: a parametric study." *Industrial & Engineering Chemistry Research* 50, no. 2 (2011): 1150-1157. https://doi.org/10.1021/ie101752z

[5] Khosravi-Bizhaem, Hamed, Abbas Abbassi, and Amir Zivari Ravan. "Heat transfer enhancement and pressure drop by pulsating flow through helically coiled tube: An experimental study." *Applied Thermal Engineering* 160 (2019): 114012. https://doi.org/10.1016/j.applthermaleng.2019.114012

[6] El-Genk, Mohamed S., and Timothy M. Schriener. "A review and correlations for convection heat transfer and pressure losses in toroidal and helically coiled tubes." *Heat Transfer Engineering* 38, no. 5 (2017): 447-474. https://doi.org/10.1080/01457632.2016.1194693

[7] Kumar, E. Pavan, Anand Kumar Solanki, and M. Mohan Jagadeesh Kumar. "Numerical investigation of heat transfer and pressure drop characteristics in the micro-fin helically coiled tubes." *Applied Thermal Engineering* 182 (2021): 116093. https://doi.org/10.1016/j.applthermaleng.2020.116093

[8] Palanisamy, K., and P. C. Mukesh Kumar. "Heat transfer enhancement and pressure drop analysis of a cone helical coiled tube heat exchanger using MWCNT/water nanofluid." *Journal of Applied Fluid Mechanics* 10, no. Special Issue) (2017): 7-13. https://doi.org/10.36884/jafm.10.SI.28265

[9] Palanisamy, K., and PC Mukesh Kumar. "Experimental investigation on convective heat transfer and pressure drop of cone helically coiled tube heat exchanger using carbon nanotubes/water nanofluids." *Heliyon* 5, no. 5 (2019). https://doi.org/10.1016/j.heliyon.2019.e01705

[10] Laohalertdecha, S., A. S. Dalkilic, and S. Wongwises. "A review on the heat-transfer performance and pressure-drop characteristics of various enhanced tubes." *International Journal of Air-Conditioning and Refrigeration* 20, no. 04 (2012): 1230003. https://doi.org/10.1142/S2010132512300030

[11] Abdullah, Mustafa Sabah, and Adnan Mohammed Hussein. "Thermal performance of a helical coil heat exchanger utilizing nanofluids: a review." *Journal of Heat and Mass Transfer Research* 10, no. 1 (2023): 121-134.

[12] Fakoor-Pakdaman, M., M. A. Akhavan-Behabadi, and P. Razi. "An empirical study on the pressure drop characteristics of nanofluid flow inside helically coiled tubes." *International Journal of Thermal Sciences* 65 (2013): 206-213. https://doi.org/10.1016/j.ijthermalsci.2012.10.014

[13] Hashemi, S. M., and M. A. Akhavan-Behabadi. "An empirical study on heat transfer and pressure drop characteristics of CuO–base oil nanofluid flow in a horizontal helically coiled tube under constant heat flux." *International Communications in Heat and Mass Transfer* 39, no. 1 (2012): 144-151. https://doi.org/10.1016/j.icheatmasstransfer.2011.09.002

[14] El-Genk, Mohamed S., and Timothy M. Schriener. "A review and correlations for convection heat transfer and pressure losses in toroidal and helically coiled tubes." *Heat Transfer Engineering* 38, no. 5 (2017): 447-474. https://doi.org/10.1080/01457632.2016.1194693

[15] Ghobadi, Mehdi, and Yuri Stephan Muzychka. "A review of heat transfer and pressure drop correlations for laminar flow in curved circular ducts." *Heat Transfer Engineering* 37, no. 10 (2016): 815-839. https://doi.org/10.1080/01457632.2015.1089735

[16] Aly, Wael IA. "Numerical study on turbulent heat transfer and pressure drop of nanofluid in coiled tube-in-tube heat exchangers." *Energy Conversion and Management* 79 (2014): 304-316. https://doi.org/10.1016/j.enconman.2013.12.031

[17] Palanisamy, K., and PC Mukesh Kumar. "Experimental investigation on convective heat transfer and pressure drop of cone helically coiled tube heat exchanger using carbon nanotubes/water nanofluids." *Heliyon* 5, no. 5 (2019). https://doi.org/10.1016/j.heliyon.2019.e01705

[18] Laohalertdecha, S., A. S. Dalkilic, and S. Wongwises. "A review on the heat-transfer performance and pressure-drop characteristics of various enhanced tubes." *International Journal of Air-Conditioning and Refrigeration* 20, no. 04 (2012): 1230003. https://doi.org/10.1142/S2010132512300030

[19] Bhuvaneswari, S., and G. Elatharasan. "Numerical study of heat transfer and pressure drop in a helically coiled tubes." *Trends in Mechanical and Biomedical Design: Select Proceedings of ICMechD 2019* (2020): 785-796. https://doi.org/10.1007/978-981-15-4488-0_66

[20] Lyudmila, Irmuhamedova, Qudratova Gulzoda, Sodiqova Nigora, Vakhidova Umida, and Gafarova Zumrad. "Computational study of helical coil heat exchangers for water systems." In *E3S Web of Conferences*, vol. 648, p. 03025. EDP Sciences, 2025. https://doi.org/10.1051/e3sconf/202564803025